

A-5-4

Influence of Extension Formation Process on Indium Halo Profile

D. Onimatsu, and K. Shibahara

Research Center for Nanodevices and Systems, Hiroshima University

1-4-2 Kagamiyama, Higashi-Hiroshima, 739-8527, Japan

Phone: +81-824-24-6265, Fax: +81-824-22-7185, e-mail: onimatsu@sxsys.hiroshima-u.ac.jp

Abstract

Halo doping is one of the key technologies for MOSFET doping design. However, Halo profile is strongly affected by the S/D (Source and Drain) formation process. We have investigated variations in Indium (In) Halo depth profiles due to differences in the S/D formation process. In order to minimize TED (Transient Enhanced Diffusion) of In, In must be implanted after S/D implantation that accompanies the formation of the amorphous layer. The mechanism of redistribution of In atoms is discussed based on SIMS (Secondary Ion Mass Spectroscopy) and TEM (Transmission Electron Microscopy) evaluations.

1. Introduction

Shallow junction formation is a necessary technology for the suppression of short-channel effects due to gate-length scaling. Halo doping underneath the S/D (Source and Drain) extensions is also effective for short-channel effect suppression[1]. For n-MOSFETs, Indium (In) Halo is superior to Boron (B) Halo for that purpose because of its steeper profile[2]. However, In sometimes displays very fast diffusion with interstitial silicon (Si) atoms, and its low thermal-equilibrium solid solubility ($2 \times 10^{17} \text{ cm}^{-3}$) easily leads to precipitation. Therefore, before and after process steps are important to prevent enhanced diffusion and/or pileup[3]. Though Halo implantation, extension implantation and annealing for the recovery of damaged crystallinity by ion implantation are sequence processes in general, their order for minimizing In diffusion has not been discussed yet. Accordingly, we have investigated how In diffusion is influenced by the permutation of these processes with very shallow, 20 nm depth junctions formed by Antimony (Sb) implantation [4].

2. Experiment

Implantation conditions for In Halo and Sb extensions are listed in Table 1. Antimony is suitable for S/D extension formation because of its low diffusive feature and low sheet resistance, as shown in the Introduction section. Arsenic (As) is used in limited cases instead of Sb for comparison. In was implanted into Si at 60 keV energy for $1 \times 10^{13} \text{ cm}^{-2}$.

In this paper, the process flow in which the In is implanted before Sb is called "In 1st" and the reverse is called "Sb 1st". Concerning rapid thermal annealing (RTA), "1 step" and "2 steps" are compared. In the former case, RTA was performed only once after the second implantation. In the latter, RTA was carried out just after each implantation. As shown in Fig. 1, samples of the Sb-1st-1-step, Sb-1st-2-steps and In-1st-1step were fabricated.

Dopant depth profiles were evaluated by SIMS analysis, and defects in the Si were observed with TEM.

3. Results

Figure 2 shows depth profiles for the Sb extension and In Halo of the Sb-1st-1-step sample. After 10 s RTA at 900°C, at the tail region of the Sb extension, In pileup is observed and profile broadening is clear at the In tail region. Depth profiles for the same implantation condition and different RTA times are shown in Fig. 3. The change in the In depth profile indicated in Fig. 2 is already observed for the spike annealing (0 s RTA) case, and further change in the profile

is very slight even after 60 s RTA. This result shows that In TED (Transient Enhanced Diffusion) has a sub-second duration, and further diffusion is quite slower than this TED. Figure 4 shows the comparison between the In-1st and Sb-1st cases. The In tail profile for the Sb-1st is slightly steeper than that for the In-1st.

Figure 5 shows the comparison between the 1-step RTA and 2-steps RTA for the Sb-1st condition. The In pileup peak found at the extension tail for the 1-step RTA is higher than that for the 2-steps RTA, and the In tail profile for the 1-step RTA is steeper than that for the 2-steps. From the point of view of the device fabrication, the Sb-1st-1-step was the best because it had the steepest In profile. These In behaviors are also observed for the As extension case as shown in Fig. 6, which implies that obtained results are not due to specific features of Sb.

4. Discussion

Cross-sectional TEM micrographs for the Sb-1st-1-step and Sb-1st-2-steps are shown in Figs. 7 and 8, respectively. Many EOR (End of Range) defects were observed in the specimen for the 1-step, as shown in Fig. 7. However, the EOR defects were not found in the cross-sectional observation for the 2-steps. In these specimens, (311) defects were not observed. This supports the sub-second TED shown in Fig. 3, because (311) defects that consist of interstitial Si gradually decompose and arise in TED.

The depth of the In pileup observed in the SIMS profile is almost the same as that of the EOR defects. In seems to aid in the formation of, and be trapped by, the EOR defects. This trapping means a decrease in mobile In atoms that is one of the considerable causes of a steeper In profile for the 1-step annealing. In addition, if the interstitial Si atoms are also trapped by the EOR defects, TED is weakened. In the case of the 2-steps annealing, EOR defect density is so small, and the loss of mobile In and interstitial Si atoms is so limited, that profile broadening in the tail region is apparent. The In diffusion model described here is summarized in Fig. 9.

5. Conclusion

The In Halo profile was evaluated in relation to the extension formation process. The In displayed very fast TED at the early stage of RTA, and the consequent diffusion was much slower. Sb implantation before In implantation effectively reduced In diffusion. The 2-steps annealing reduced the EOR defects; however, In diffusion was apparent. Consequently, the best process order for obtaining a steep In profile was extension implantation, Halo implantation and RTA.

Acknowledgment

Part of this work was supported by a Grant-in-aid for Scientific Research (C) from the Ministry of Education, Science, Sports and Culture.

Reference

- [1] K. Miyashita et al., *IEDM Tech. Dig.*, 1999, pp.649-652.
- [2] K. Nakanishi et al., *SSDM Ext. Abst.*, 1999, pp.116-117.
- [3] T. Matsuda et al., *SSDM Ext. Abst.*, 2000, pp.18-19.
- [4] K. Shibahara et al., *Mater. Res. Soc. Symp. Proc.*, 2000, vol. 610, pp. B8.5.1-B8.5.6.

Table.1: (a) Implantation conditions for In Halo and Sb extension. (b) RTA condition for 1-step and 2-steps RTA.

(a)				(b)			
	Energy [keV]	Dose [cm ⁻²]	Tilt Angle [degree]		Temperature [°C]	Time [s]	
In Halo	60	1x10 ¹³	30	1-step RTA			
Sb extension	10	3x10 ¹⁴	7	2-steps RTA	1st	900	10
					2nd	900	10

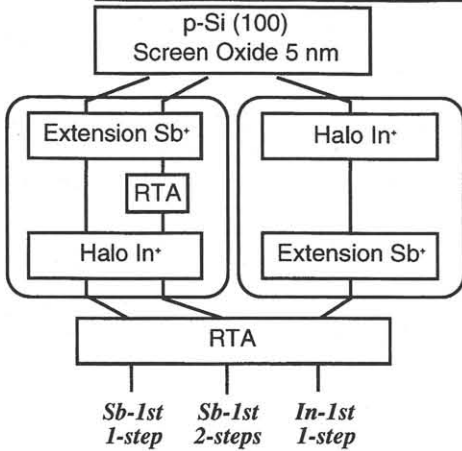


Fig. 1 Extension and Halo formation process flow.

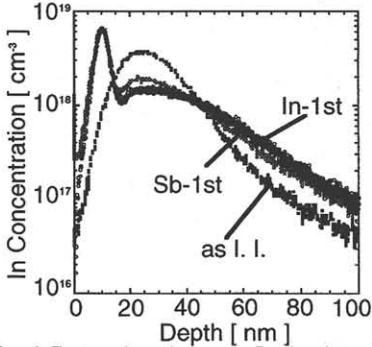


Fig. 4 Comparison between In depth profiles for Sb-1st and In-1st. Both are 1-step RTA.

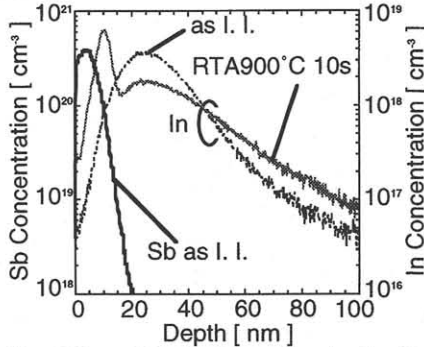


Fig. 2 Sb and In depth profiles for the Sb-1st-1-step case. The In profile after RTA shows its pileup at the Sb tail depth and tail broadening.

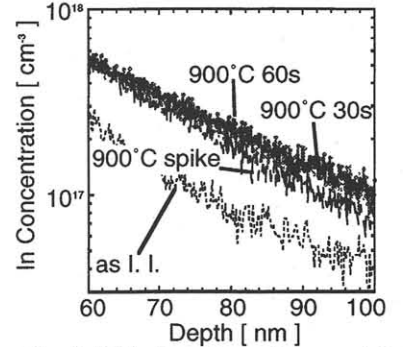


Fig. 3 RTA time dependence of In depth profiles for the same implantation condition as Fig. 1.

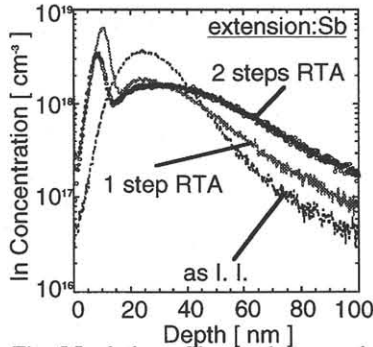


Fig. 5 In dpth profiles for 1-step and 2-steps RTA using Sb-1st condition.

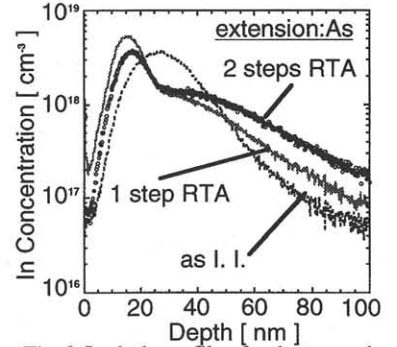


Fig. 6 In dpth profiles for 1 step and 2 step RTA for As extension.

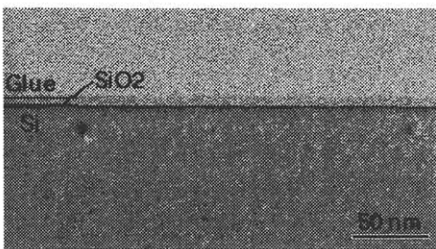


Fig. 7 A cross-sectionnal TEM micrograph of Sb-1st-1-step.

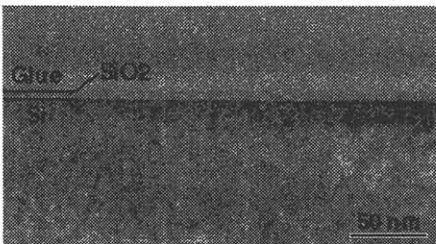
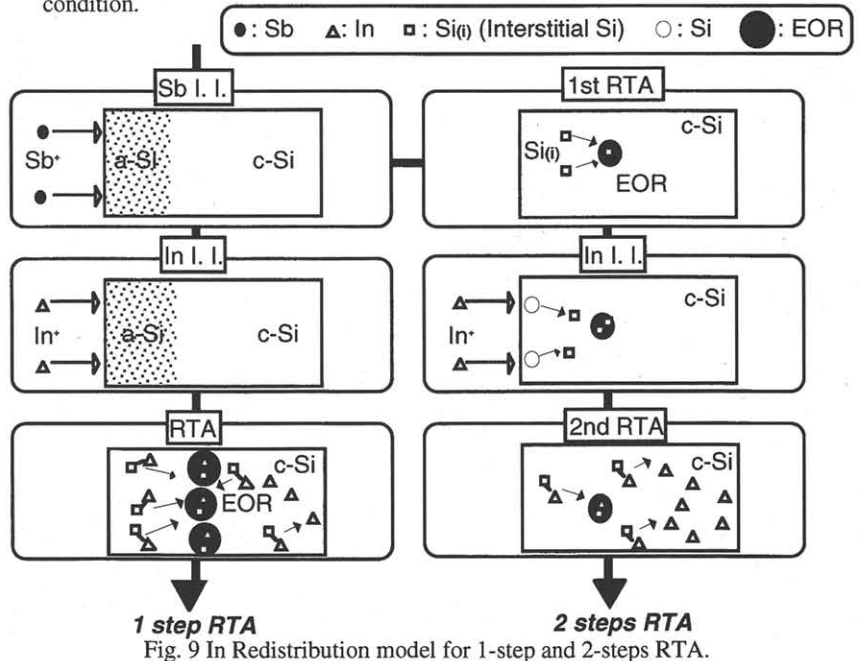


Fig. 8 A cross-sectionnal TEM micrograph of Sb-1st-2-steps.



1 step RTA

2 steps RTA

Fig. 9 In Redistribution model for 1-step and 2-steps RTA.